ORIGINAL ARTICLE

Radiosensitization of the Gold, Silver, and Gadolinium Nanoparticles in ^{177}Lu Radionuclide Radiation Field in Microscopic and Macroscopic Scales in the Liver Radionuclide Therapy

Wrya Parwaie [1], Mikaeil Molazadeh [2,3*], Tohid Mortezazadeh [2,3*], Hosein Ghiasi [2]

[1] *Department of Medical Physics, Faculty of Paramedical Sciences, Ilam University of Medical Sciences, Ilam, Iran*

[2] *Medical Radiation Sciences Research Center, Tabriz University of Medical Sciences, Tabriz, Iran*

[3] *Department of Medical Physics, Faculty of Medicine, Tabriz University of Medical Sciences, Tabriz, Iran*

*Corresponding Authors: Mikaeil Molazadeh, Tohid Mortezazadeh
Emails: mikaeel.mollazadeh@gmail.com, tmortezazadeh@gmail.com

Received: 15 March 2025 / Accepted: 25 May 2025

Abstract

Purpose: The purpose of this study was to estimate the dose enhancement of Gold, Silver, and Gadolinium on both microscopic and macroscopic scales in liver ^{177}Lu nano-radionuclide therapy.

Materials and Methods: The ^{177}Lu radionuclide at the nano-scale was simulated using the MCNP 6.1 Monte Carlo (MC) simulation method. The emitted radiation characteristics, such as type and energy of emitted radiation, were modeled at the center of the tumor. The tumor cell (phantom liver) was filled with cubic voxels with sides of 1µm. These cubic voxels were then filled with GNP, AgNP, and GdNP spherical nanoparticles with a diameter of 30 nm each, and in a concentration of 10 mg/g of tissue.

Results: The DEF was estimated at 5µm, 20µm, 50µm, 70µm, and 100µm from a single ^{177}Lu nano-radionuclide radiation source at the center of the phantom liver cell, emitting both γ-ray and β- particles. A significant γ-ray DEF of up to 89% was observed at some µm around the source. Additionally, high DEF was derived for β- rays at some µm around the simulated radionuclides compared to greater distances. Estimated DEF in tumoral tissue including GNP was 89%, 78%, 72%, 47%, and 25% at 5µm, 20µm, 50µm, 70µm, and 100µm respectively from the center. DEF for the other nanoparticles was also derived.

Conclusion: A dramatic DEF was observed in the close vicinity of NPs around ^{177}Lu as the radiation source, possibly due to the great gradient in dose and dominance of the photo-electric phenomenon.

Keywords: Monte Carlo; Radionuclide; Dose Enhancement; Nanoparticle.

DOI: https://doi.org/10.18502/fbt.v12i3.19173

1. Introduction

Nowadays, the use of radiation therapy modalities such as linear electron accelerators (linacs) megavoltage electron and photon beams radiation therapy, brachytherapy, and radionuclide therapy have been approved as standard methods in cancer treatment. Skidmore *et al.* [1] conducted a study and compared High-Dose-Rate (HDR) brachytherapy to linac-based external radiotherapy. They found that HDR brachytherapy is more effective at sparing the rectum, bladder, and urethra from excess doses while delivering a higher dose to the prostate. Additionally, adding non-toxic and high Z metal nanoparticles to tumoral tissue increases the absorbed dose due to the physical characteristics of the nanoparticles. These nanoparticles have a high Z and are non-toxic, with a prevalence of photoelectric effects at low energies that produce short-range photoelectrons [2-8]. In the literature, the addition of some percentages of the Gold Nanoparticles (GNP) [2, 9- 11], Siver nanoparticles (AgNPs) [4, 12, 13], and gadolinium nanoparticles (GdNPs) [4, 14-16] were carried out to derive Dose Enhancement (DE) due to the nanoparticles (NPs) by the researchers [17]. Ghasemi-Jangjoo and Ghiasi [17] utilized GNPs and GdNPs to enhance the radiation dose in the field of ^{125}I brachytherapy seeds. It was reported that the DE for GNPs was two times higher than that for GdNPs. McMahon *et al.*, simulated 2 nm GNPs and estimated Dose Enhancement Factor (DEF) using nanodosimetry. They compared the results to experimental data and the main conclusion of their study was reported as finding a significant increase in DEF, which they attributed to the effects of high dose inhomogeneity and local dose deposition, as studied by the LEM. The results were consistent with the experiment, suggesting sub-cellular localization, which is crucial in estimating the high DEF of GNPs [18]. In another study, McMahon *et al.* [19] examined the impact of radiation on the DE of GNPs and found that DE occurs at low energies. The significant DE of GNPs in radiation therapy compared to other nanoparticles prompted an investigation into the size, geometry, energy, and other parameters that affect the physics of GNP dose enhancement. Cellular DE factors in medical nuclear energy settings are influenced by the modeling of GNPs, with a notable difference observed. The researchers simulated a hexagonal lattice of GNPs, incorporating voxels for the most realistic modeling possible. Across all simulations of the cell and nucleus radius were some μm cell, nuclear, and maximum cellular DE reported as 6.83 times [20]. MC code calculation was conducted by Ramonaheng *et al.* [21] and in an in-vivo dosimetry a high DEF was obtained for the bismuth oxide NPs with a high concentration in the tumor that was irradiated with a ^{137}C source to estimate DE due to bismuth oxide NPs [22]. According to Taha *et al.* [12], the DEF was estimated for AgNPs with high concentrations at 12.55 in the vicinity of ^{125}I seed, which was higher than the dose enhancement of 103Pd and 198Au under the same conditions, respectively. Fuentealba *et al.* [15] also investigated the DE deu to NPs in the radiation fields. There are enormous publications on the NPs' radiosensitization and DE due to different NPs in the literature [4, 12, 14, 15, 17, 21-23]. In the current study, the authors aimed to estimate microscopic and macroscopic DEF for GNP, GdNP, and AgNP around the ^{177}Lu nano-radionuclide emitted γ-ray and β- particles in the liver nano-radionuclide therapy. It should be studied that, we estimated DEF for both γ-ray and β- particles separately in the phantom liver cell. Dose, fluence, and emitted radiation from the ^{177}Lu nano-radionuclide, both γ-ray and β- particles scored separately.

2. Materials and Methods

In the current study, the MCNP version 6.1 Monte Carlo simulation code was utilized for simulations and calculations. The MCNP code incorporated various capabilities such as simulating complex geometries, intricate radiation physics, and diverse problem modeling. Rich physical cross-section libraries were also employed. For the calculations, a cubic voxel was filled with NPs of 30 nm in diameter, including GNP, AgNP, and GdNPs separately in a tumor phantom with sides of 1 μm. Subsequently, a tumor filled with 10 mg/g of NPs in tumor in the liver tissue density of 1.016 g/cm^3 was simulated. Lutetium (^{177}Lu) nano-radionuclide was used as the radiation source in this study, modeled in a 100 nm microsphere with specific energy characteristics. The decay mode of ^{177}Lu emits beta particles with maximum energies of 497 keV, 384 keV, and 176 keV, along with low-energy gamma-rays at 113 keV and 208 keV. To model GNP with gamma rays, a high Specific Activity (SA) value

exceeding 740 GBq of ^{177}Lu was required for optimal effect. A lattice configuration was created using the MCNP 6.1 MC code, with a 100 nm diameter NP positioned in the center of each cubic voxel within the tumor-modeled cell inside the phantom for the NPs studied, as shown in Figure 1. The interaction of γ-rays with lower energy results in photoelectric effects and ejected photo-electrons, with short-range electrons depositing their energies close to the production origin. This local enhancement by high Linear Energy Transfer (LET) electrons from the NPs is beneficial for cancer treatment. Beta-rays, with short range and high LET, are suitable for treating metastatic sites like liver metastasis and organ cancer. The study focused on microdosimetric and macroscopic DEF to increase sensitivity at the cellular level using the MCNP 6.1 MC code. The LEM near the NPs created significant dose inhomogeneities around the NPs exposed to radiation, resulting in a notable dose gradient. Microscopic and macroscopic DEF were estimated using MC code calculations with ^{177}Lu nano-radionuclide for potential clinical application in liver cancer treatment. Local DE with short-range electrons was utilized to target and remove liver metastasis. The DEF within a few micrometers around ^{177}Lu close to a single nano-scale GNP was reported in the results section.

3. Results

For GNPs DEF obtaining, a higher value of F1 tally that scores current integrated over a surface obtained 1.68×10^{-5} particles at a surface positioned 5µm from the radionuclide. F2 calculating flux averaged a surface maximum value derived as 19.63×10^{3} cm^{-2} at the surface at a distance of 5µm from the source. F4 tally which scores flux averaged over a cell higher value of 17.99×10^{3}particles per cm^{-2} and by the use of *F8 tally, MC code scored energy deposition at the cell in MeV. The highest value of the energy deposition was 16.98 $\times10^{-7}$ MeV. Using *F8 tallied value in water and GNP included water DEF at 5µm from the radiation source was derived as 89%. The same values scored by tallies were shown in Table 1b and values obtained in GNP included water in a concentration of 10mg/g and diameter of 30nm. From Tables 1a and 1b, scoring doses in water and simulated water cell, including GNPs, DEF was estimated from 5µm to 100µm as 89%, 78%, 72%, 47%, and 25% at 5µm, 20µm, 50µm, 70µm, and 100µm, respectively. Tables 1c and 1d indicated microscopic DEF at the same distances from the radiation source derived by MCNP 6.1 as 67%, 66%, 42%, 37%, and 38% at 5µm, 20µm, 50µm, 70µm, and 100µm, respectively. The values were for silver or AgNPs DEF as a nontoxic and high Z metal. For GdNPs, DEF was obtained at

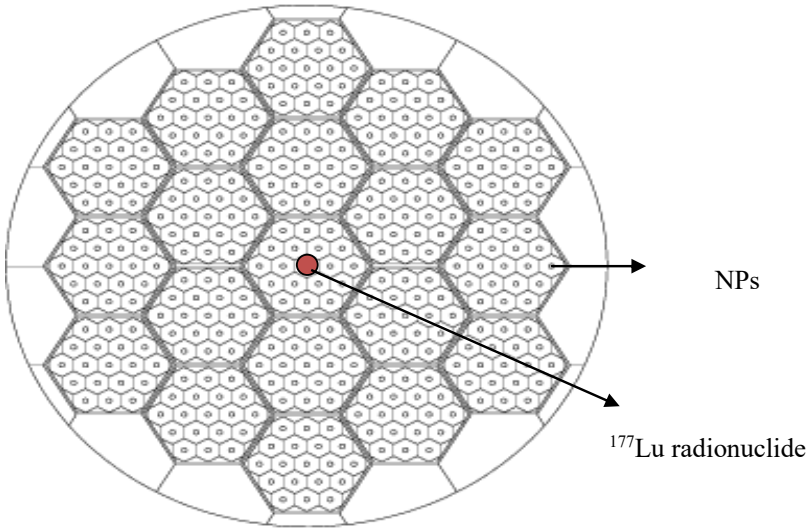

Figure 1. MCNP 6.1 simulated lattice configuration, and created voxels with an NP in the voxel center

Table 1 (a). MCNP6 MC code calculated results for the ^{177}Lu nano-radionuclide without Nano-Particle in the water phantom per source emission at 5μm to 100 μm from the ^{177}Lu source

Distance from source (μm)	F1 Tally (for γ-ray) (Number)	F2 Tally (for γ-ray) (Number/cm^2)	F4 Tally (for γ-ray) (Number/cm^2)	*F8 Tally (for γ-ray) (MeV)
5	7.45×10^{-6}	8.93×10^{3}	8.08×10^{3}	8.98×10^{-7}
20	2.84×10^{-8}	1.11×10^{2}	1.21×10^{2}	2.02×10^{-9}
50	2.31×10^{-8}	8.31×10^{1}	9.71×10^{1}	1.02×10^{-9}
70	1.98×10^{-9}	5.18×10^{1}	7.91×10^{1}	1.21×10^{-9}
100	1.01×10^{-8}	3.40×10^{1}	6.81×10^{1}	7.21×10^{-10}
Distance from source (μm)	**F1 Tally (for β^{-1}ray) Number**	**F2 Tally (for β^{-1}ray) (Number/cm^2)**	**F4 Tally (for β^{-1}ray) (Number/cm^2)**	***F8 Tally (for β^{-1}ray) (MeV)**
5	9.81×10^{-6}	5.01×10^{4}	1.18×10^{4}	9.01×10^{-5}
20	3.33×10^{-8}	3.71×10^{4}	8.77×10^{3}	8.23×10^{-7}
50	1.45×10^{-8}	2.41×10^{4}	7.69×10^{3}	6.79×10^{-7}
70	9.03×10^{-9}	1.65×10^{4}	6.30×10^{3}	5.00×10^{-7}
100	8.00×10^{-9}	1.21×10^{4}	4.12×10^{3}	3.89×10^{-7}

Table 1 (b). MCNP6 MC code calculated results for the ^{177}Lu nano-radionuclide with GNPs in the water phantom per source emission at 5μm to 100 μm from the ^{177}Lu source

Distance from source(μm)	F1 Tally (for γ-ray) (number)	F2 Tally (for γ-ray) (number/cm^2)	F4 Tally (for γ-ray) (number/cm^2)	*F8 Tally (for γ-ray) (MeV)
5	1.68×10^{-5}	19.63×10^{3}	17.99×10^{3}	16.98×10^{-7}
20	7.84×10^{-8}	9.23×10^{2}	8.56×10^{2}	3.61×10^{-9}
50	5.11×10^{-8}	16.51×10^{1}	2.03×10^{2}	1.76×10^{-9}
70	3.98×10^{-9}	10.43×10^{1}	18.87×10^{1}	17.01×10^{-10}
100	2.35×10^{-9}	5.23×10^{1}	15.74×10^{1}	11.03×10^{-10}
Distance from source(μm)	**F1 Tally (forβ^{-1}ray)(number)**	**F2 Tally (forβ^{-1}ray)**	**F4 Tally (forβ^{-1}ray) (number/cm^2)**	***F8 Tally (forβ^{-1}ray) (MeV)**
5	15.99×10^{-6}	9.98×10^{4}	3.12×10^{4}	11.76×10^{-5}
20	10.34×10^{-8}	8.78×10^{4}	16.98×10^{3}	10.66×10^{-7}
50	11.21×10^{-8}	5.21×10^{4}	15.67×10^{3}	8.32×10^{-7}
70	16.88×10^{-9}	3.88×10^{4}	13.34×10^{3}	6.02×10^{-7}
100	17.77×10^{-9}	2.04×10^{4}	7.00×10^{3}	4.87×10^{-7}

Table 1 (c). MCNP6 MC code calculated results for the ^{177}Lu nano-radionuclide in the water phantom per source emission at 5μm to 100 μm from the ^{177}Lu source

Distance from source(μm)	F1 Tally (for γ-ray) (number)	F2 Tally (for γ-ray) (number/cm^2)	F4 Tally (for γ-ray) (number/cm^2)	*F8 Tally (for γ-ray) (MeV)
5	7.45×10^{-6}	8.93×10^{3}	8.08×10^{3}	8.98×10^{-7}
20	2.84×10^{-8}	1.11×10^{2}	1.21×10^{2}	2.02×10^{-9}
50	2.31×10^{-8}	8.31×10^{1}	9.71×10^{1}	1.02×10^{-9}
70	1.98×10^{-9}	5.18×10^{1}	7.91×10^{1}	8.98×10^{-10}
100	1.01×10^{-8}	3.40×10^{1}	6.81×10^{1}	7.21×10^{-10}
Distance from source(μm)	**F1 Tally (forβ^{-1}ray) (number)**	**F2 Tally (forβ^{-1}ray) (number/cm^2)**	**F4 Tally (forβ^{-1}ray) (number/cm^2)**	***F8 Tally (forβ^{-1}ray)**
5	9.81×10^{-6}	5.01×10^{4}	1.18×10^{4}	9.01×10^{-5}
20	3.33×10^{-8}	3.71×10^{4}	8.77×10^{3}	8.23×10^{-7}
50	1.45×10^{-8}	2.41×10^{4}	7.69×10^{3}	6.79×10^{-7}
70	9.03×10^{-9}	1.65×10^{4}	6.30×10^{3}	5.00×10^{-7}
100	8.00×10^{-9}	1.21×10^{4}	4.12×10^{3}	3.89×10^{-7}

Table 1 (d). MCNP6 MC code calculated results for the ^{177}Lu nano-radionuclide with AgNPs in the water phantom per source emission at 5μm to 100 μm from the ^{177}Lu source

Distance from source(μm)	F1 Tally (for γ-ray) (number)	F2 Tally (for γ-ray) (number/cm^2)	F4 Tally (for γ-ray) (number/cm^2)	*F8 Tally (for γ-ray) MeV
5	15.45×10^{-6}	15.01×10^{3}	14.98×10^{3}	14.98×10^{-7}
20	7.45×10^{-8}	2.01×10^{2}	2.00×10^{2}	3.39×10^{-9}
50	5.00×10^{-8}	15.04×10^{1}	16.08×10^{1}	2.67×10^{-9}
70	4.01×10^{-9}	9.44×10^{1}	13.00×10^{1}	12.32×10^{-10}
100	1.40×10^{-9}	5.65×10^{1}	10.33×10^{1}	10.01×10^{-10}
Distance from source(μm)	**F1 Tally (for β^{-1}ray) (number)**	**F2 Tally (for β^{-1}ray) (number/cm^2)**	**F4 Tally (for β^{-1}ray) (number/cm^2)**	***F8 Tally (for β^{-1}ray)**
5	15.09×10^{-6}	11.87×10^{4}	2.89×10^{4}	13.67×10^{-5}
20	7.54×10^{-8}	7.86×10^{4}	15.32×10^{3}	11.89×10^{-7}
50	3.02×10^{-8}	4.00×10^{4}	9.99×10^{3}	11.45×10^{-7}
70	17.23×10^{-9}	3.01×10^{4}	10.31×10^{3}	6.74×10^{-7}
100	14.99×10^{-9}	2.75×10^{4}	7.01×10^{3}	5.76×10^{-7}

Table 1 (e). MCNP6 MC code calculated results for the ^{177}Lu nano-radionuclide in the water phantom per source emission at 5μm to 100 μm from the ^{177}Lu source

Distance from source(μm)	F1 Tally (for γ-ray) (number)	F2 Tally (for γ-ray) (number/cm^2)	F4 Tally (for γ-ray) (number/cm^2)	*F8 Tally (for γ-ray)(MeV)
5	7.45×10^{-6}	8.93×10^{3}	8.08×10^{3}	8.98×10^{-7}
20	2.84×10^{-8}	1.11×10^{2}	1.21×10^{2}	2.02×10^{-9}
50	2.31×10^{-8}	8.31×10^{1}	9.71×10^{1}	1.02×10^{-9}
70	1.98×10^{-9}	5.18×10^{1}	7.91×10^{1}	8.98×10^{-10}
100	1.01×10^{-8}	3.40×10^{1}	6.81×10^{1}	7.21×10^{-10}
Distance from source(μm)	**F1 Tally (forβ^{-1}ray) (number)**	**F2 Tally (forβ^{-1}ray) (number/cm^2)**	**F4 Tally (forβ^{-1}ray) (number/cm^2)**	***F8 Tally (forβ^{-1}ray) (MeV)**
5	9.81×10^{-6}	5.01×10^{4}	1.18×10^{4}	9.01×10^{-5}
20	3.33×10^{-8}	3.71×10^{4}	8.77×10^{3}	8.23×10^{-7}
50	1.45×10^{-8}	2.41×10^{4}	7.69×10^{3}	6.79×10^{-7}
70 μm	9.03×10^{-9}	1.65×10^{4}	6.30×10^{3}	5.00×10^{-7}
100 μm	8.00×10^{-9}	1.21×10^{4}	4.12×10^{3}	3.89×10^{-7}

Table 1 (F). MCNP6 MC code calculated results for the ^{177}Lu nano-radionuclide with GdNPs in the water phantom per source emission at 5μm to 100 μm from the ^{177}Lu source

Distance from source(μm)	F1 Tally (for γ-ray) (number)	F2 Tally (for γ-ray) (number/cm^2)	F4 Tally (for γ-ray) (number/cm^2)	*F8 Tally (for γ-ray)(MeV)
5	9.97×10^{-6}	14.31×10^{3}	9.98×10^{3}	15.98×10^{-7}
20	5.67×10^{-8}	3.45×10^{2}	2.09×10^{2}	3.59×10^{-9}
50	5.56×10^{-8}	14.23×10^{1}	12.34×10^{1}	1.41×10^{-9}
70	2.64×10^{-9}	9.66×10^{1}	9.21×10^{1}	15.63×10^{-10}
100	2.34×10^{-9}	7.67×10^{1}	8.98×10^{1}	9.89×10^{-10}
Distance from source (μm)	**F1 Tally (forβ^{-1}ray)(number)**	**F2 Tally (forβ^{-1}ray) (number/cm^2)**	**F4 Tally (forβ^{-1}ray) (number/cm^2)**	***F8 Tally (forβ^{-1}ray) (MeV)**
5	14.87×10^{-6}	12.94×10^{4}	3.01×10^{4}	11.46×10^{-5}
20	6.97×10^{-8}	6.66×10^{4}	16.22×10^{3}	11.01×10^{-7}
50 μm	3.76×10^{-8}	5.32×10^{4}	14.56×10^{3}	9.87×10^{-7}
70 μm	17.00×10^{-9}	3.86×10^{4}	11.39×10^{3}	6.68×10^{-7}
100 μm	8.43×10^{-9}	2.56×10^{4}	9.75×10^{3}	4.65×10^{-7}

5µm, 20µm, 50µm, 70µm, and 100µm as 77%, 54%, 40%, 37%, and 34%. From the results of DEF for the studied NPs, GNPs associated with the highest DEF and AgNPs showed lower DEF, and GdNPs DEF was between the highest and lowest. From the nano-scale radionuclide of ^{177}Lu, the electron dose increases to local DE, which was shown in Tables 1a to 1f. The results indicated that DEF was due to GNPs, AgNPs, and GdNPs being lower compared to photon DEF. In the electron DEF also GNPs and AgNPs were the maximum and minimum DEF while GdNPs DEF were between the GNPs and AgNPs DEFs. From the results, it was observed that at 5, 20, 50, 70, and 100µm from the source, microscopic DEF (mDEF) for the NPs derived and at 5µm to 100µm for the studied NPs mentioned above. Macrodosimetric DEFs were seen in distances of 2cm compared to 1cm from the source a small value of 1.03 times or 3%. The generated electrons range in water was 13 mm and the high LET of the electrons shouldn't be expected compared to the close vicinities to the source. Comparing the results to the DEFs due to megavoltage accelerators that are on average of 1.01 to 1.04 (1% and 4%) and microdosimetric radiosensitizer effect due to the studied NPs, is dramatically high, and significant inhomogeneity may be the cause of such high DEF [18]. Finally, in the current study, a single GNP in the ^{177}Lu radionuclide radiation field enhanced the dose up to 89% in 5µm from the source on the microscopic scale, and at 1cm-2cm from the radiation source, the radiation dose enhanced as 3% on the macroscopic scale. Figures 2 and 3 show estimated characteristics of β^- and γ-ray, respectively, such as the number of β^- and γ-ray number at voxels, crossing β^- particles and γ-ray photons on the surfaces, and fluence of the radiations at the voxels.

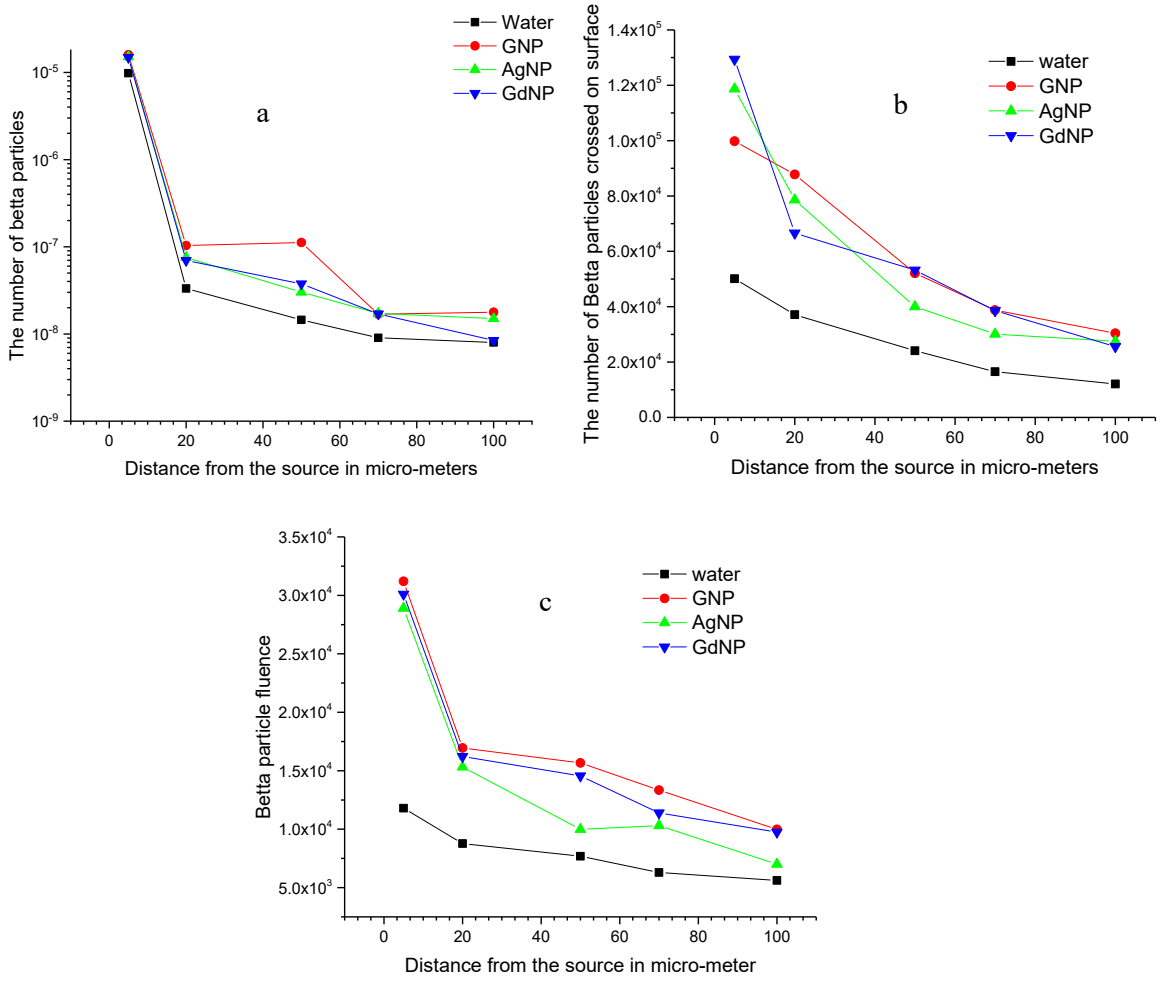

Figure 2. (a): The number of betta particles scored by MCNP code of the MC simulation in some micro-meters around the source. (b): MCNP MC simulation code derived the number of betta crossings on the surface of some micro-meters around the source (Particle flux). (c): MCNP MC simulation code derived betta particle fluence at voxels some micro-meters around the source

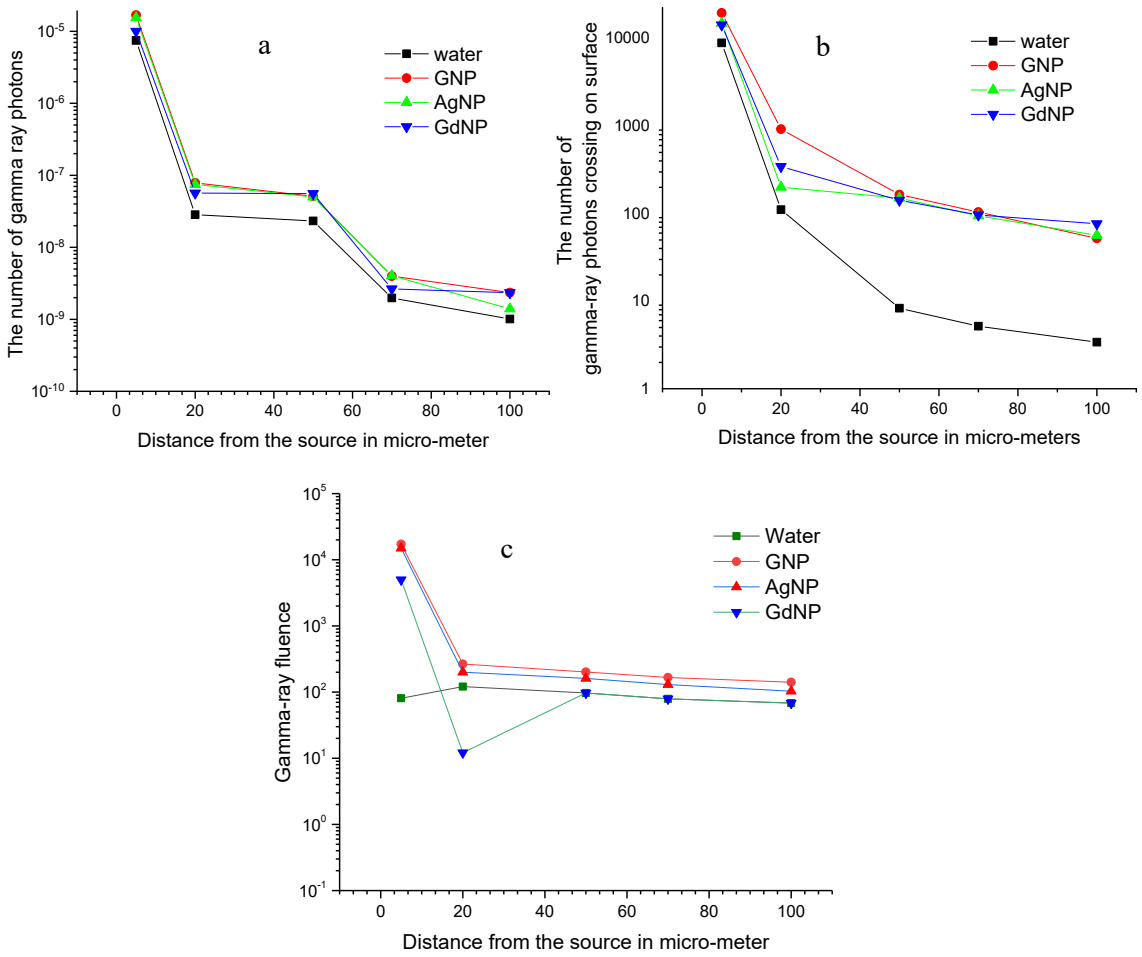

Figure 3. (a). MCNP MC simulation code derived photon numbers at some micro-meters around the the source. (b). MCNP MC simulation estimated photons crossing on the surfaces at some micro-meters around the source. (c). MCNP MC simulation code derived photons fluence at the voxels at some micro-meters around the source

4. Discussion

Our results in DEF by GNPs, GdNPs, and, AgNPsis are shown in Figure 4. According to Figure 4, GNPs enhanced the dose higher compared to two NPs studied in the current study. Additionally, GdNPs DEF is higher than AgNPs. GNP microdisimetric DEF agreed with others' work results. Absorbed dose and DEF in our study agree with McMahon in the nanodosimetric study with megavoltage and high DEF can be described as LEM and dramatic DEF closer to the ^{177}Lu agreed with the McMahon's work [18]. Zabihzadeh *et al.* [24] used low-energy photon beams of 35, 55, 75, and 95 keV energy, and higher DE was reported in 55 keV. They attributed this effect to the inhomogeneity of the radiation-absorbing medium.

Their result agrees with McMahon's work that studied nanodosimetric DE due to GNP and reported high inhomogeneity as a dramatic DEF cause [18] and our study in GNP, AgNP, and GdNP DEF. Additionally, Zabihzadeh *et al.* [25] carried out a study to estimate DE and used 10mg/g which in the current study was used for an NP concentration of average of 2.17, with a maximum and minimum of DEF as 2.70 and 2.05, respectively. For the inhomogeneity medium, they estimated the average, maximum, and minimum of DEF as 2.42 for 55 keV and 4.17 and 0.96, respectively. Dramatic DEF obtained in their work was due to low energy photon beam and inhomogeneity of the medium that agrees with our results and McMahon's study [18]. They attributed the observed differences in DEF to the medium homogeneity and inhomogeneity. Our results were obtained in a homogeneity medium and in addition to

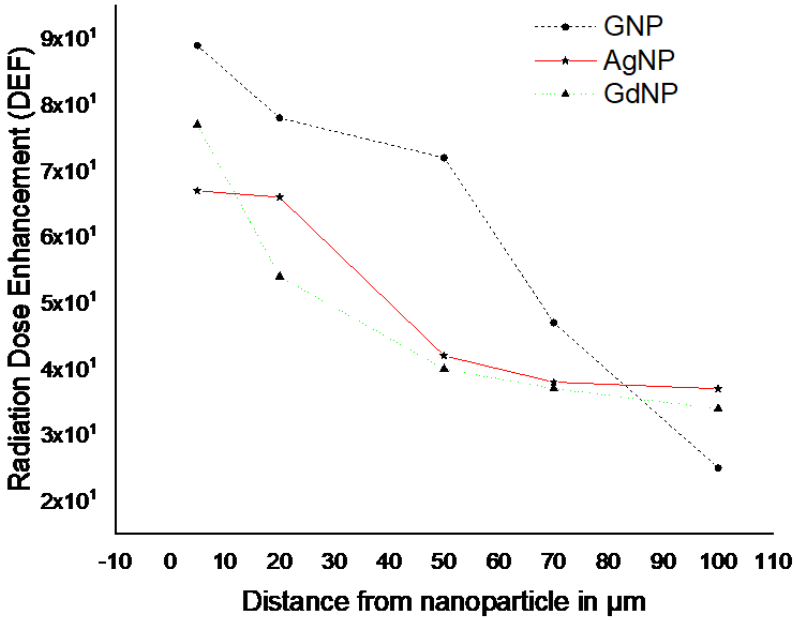

Figure 4. Dose enhancement in micro-scale by GNP, GdNP, and AgNP from NPs to 100 µm of ^{177}Lu nano-radionuclide derived by MC simulation

DEF, the flux of photons over the surface and cell and fluence of the photons increasing in 5µm, 20µm, 50µm, 70µm, and 100µm distances from the ^{177}Lu radionuclide. Also, β – rays emitted from the ^{177}Lu radionuclide, DEF, the flux of photons over the surface and cell, and fluence of the β-ray. Table 1a to Table 1f show the increase of the flux of photons over the surface and cell and the fluence of the β--ray. From the results shown in the Tables, DEF was not dramatically the same as photons DEF, but increasing in the flux of photons over the surface and cell and the fluence of the β-ray were significant. The DE of 27% and 37% for 1 and 0.5µm around ^{192}Ir brachytherapy seed respectively in the Hsing *et al.*'s [26] study and the results revealed decreasing scoring site diameter (surface), leading to rapid fall-of in the Local Dose Enhancement (LDE) that is useful in the metastatic sites of the cancerous organ such as the liver. Their DEF agreed with our obtained DEF of ^{177}Lu β-ray caused by GNP. Their conclusion was that although DEF by GNP according to GNP size and concentration, Radiation Biologic Effect (RBE), and DE were verified near the gold-tissue interface. Our β-ray DEF at 5µm agrees with the studied results by Hsing *et al.* [26]. Microdosimetric and radiobiological effects of gold nanoparticles at therapeutic radiation energies were investigated by Rabus *et al.* [27] and GNP dose enhancement was studied. In some studies, the DE obtained from the sources in µm scale and their results were in agreement with ours and verified our modeling [28, 29]. Our results revealed that atom Z has a significant effect on DEF because, in the studied energies of radiation, photo-electric occurs more than other physical phenomena, and it is proportional to Z^3 in the same energy. The authors recommend in low energies, the use of high Z (and non-toxic) NPs to DE. The short-range electrons released in photo-electric (photoelectrons) can increase LDE and, the LED removes metastatic regions in the cancerous organs such as liver metastasis.

5. Conclusion

The authors concluded that the atomic number (Z) of the applied NPs for DE plays a significant role at the same energy and distance. In this study, GNP enhanced dose more than GdNP, AgNP, and DEP. It was observed that GdNP resulted in higher DE compared to AgNP. From the results of this study, it can be concluded that in low-energy photon beams or gamma rays, the use of high Z metal NPs enhances dose more than low Z material NPs. It is also important to note that the toxicity of the applied NPs should be assessed.

Acknowledgment

The authors would like to express their deepest gratitude to Tabriz University of Medical Sciences.

The Research Ethics Committees of Vice-Chancellor in Research Affairs-Tabriz University of Medical Sciences approved the study protocol (Ethic code: IR.TBZMED.VCR.REC.1403.339).

Financial support was provided by Vice-Chancellor in Research Affairs-Tabriz University of Medical Sciences [Grant Number: 76017].

References

1- Thomas B Skidmore, Jessica Russell, Josh Bryant, Steve Alder, and John K Hayes, "Dosimetric Comparison of High-Dose-Rate Brachytherapy, Helical Tomotherapy and Linac-Based Intensity Modulated Radiaiton Therapy for Definitive Localized Prostate Cancer Treatment." *Brachytherapy,* Vol. 13p. S70, (2014).

2- Sepehr Batooei, Amir Moslehi, and Jalil Pirayesh Islamian, "A study on radiation interactions, dose enhancement, and hydrolysis with metallic nanoparticles irradiated by 6 megavoltage X-rays: Geant4 Monte Carlo simulation." *Nuclear Instruments and Methods in Physics Research Section B: Beam Interactions with Materials and Atoms,* Vol. 526pp. 19-28, (2022).

3- Tara Gray *et al.*, "A detailed experimental and Monte Carlo analysis of gold nanoparticle dose enhancement using 6 MV and 18 MV external beam energies in a macroscopic scale." *Applied Radiation and Isotopes,* Vol. 171p. 109638, (2021).

4- Mantvydas Merkis *et al.*, "Investigation of dose sensitivity and dose enhancement effect in silver nanoparticle enriched dose gels." *Radiation Physics and Chemistry,* Vol. 213p. 111213, (2023).

5- Nooshin Banaee, "Enhanced dose measurement of zinc oxide nanoparticles by radiochromic polymer dosimeter and Monte Carlo simulation." *Reports of Practical Oncology and Radiotherapy,* Vol. 25 (No. 4), pp. 515-20, (2020).

6- Hamid Reza Baghani and Shiva Nasrollahi, "Efficacy of various nanoparticle types in dose enhancement during low energy X-ray IORT: A Monte Carlo simulation study." *Radiation Physics and Chemistry,* Vol. 183p. 109432, (2021).

7- H Rabus *et al.*, "Intercomparison of Monte Carlo calculated dose enhancement ratios for gold nanoparticles irradiated by X-rays: Assessing the uncertainty and correct methodology for extended beams." *Physica Medica,* Vol. 84pp. 241-53, (2021).

8- Samaneh Hashemi, Seyed Mahmoud Reza Aghamiri, Ramin Jaberi, and Zahra Siavashpour, "An in silico study on the effect of host tissue at brachytherapy dose enhancement by gold nanoparticles." *Brachytherapy,* Vol. 20 (No. 2), pp. 420-25, (2021).

9- Nema Bassiri *et al.*, "Film-based measurement of gold nanoparticle dose enhancement for 192Ir." *Medical physics,* Vol. 47 (No. 1), pp. 260-66, (2020).

10- Ross I Berbeco, Alexandre Detappe, Panogiotis Tsiamas, David Parsons, Mammo Yewondwossen, and James Robar, "Low Z target switching to increase tumor endothelial cell dose enhancement during gold nanoparticle-aided radiation therapy." *Medical physics,* Vol. 43 (No. 1), pp. 436-42, (2016).

11- Chun-Hui Hsing, I-Chun Cho, Tsi-Chian Chao, Ji-Hong Hong, and Chuan-Jong Tung, "GNP enhanced responses in microdosimetric spectra for 192Ir source." *Radiation Measurements,* Vol. 118pp. 67-71, (2018).

12- Eslam Taha, Fathi Djouider, and Essam Banoqitah, "Monte Carlo simulation of dose enhancement due to silver nanoparticles implantation in brain tumor brachytherapy using a digital phantom." *Radiation Physics and Chemistry,* Vol. 156pp. 15-21, (2019).

13- Fraylenin Pinto Capia and Eder Jose Guidelli, "Enhanced thermoluminescence, radioluminescence, and optically stimulated luminescence from lithium fluoride and silver nanoparticles composites." *Optical Materials: X,* Vol. 21p. 100287, (2024).

14- Denis A Margalik *et al.*, "Prolonged Circulating Lipid Nanoparticles Enabled by High-Density Gd-DTPA-Bis (Stearylamide) for Long-Lasting Enhanced Tumor Magnetic Resonance Imaging." *Bioconjugate Chemistry,* Vol. 33 (No. 11), pp. 2213-22, (2022).

15- M Fuentealba and M Santibáñez, "Monte Carlo evaluation of the dose sparing and dose enhancement by combination of Gd-infused tumor and 241Am source for an endocavitary brachytherapy geometry." *Applied Radiation and Isotopes,* Vol. 163p. 109194, (2020).

16- M Santibáñez, Y Guillen, D Chacón, RG Figueroa, and M Valente, "Feasibility of dose enhancement assessment: Preliminary results by means of Gd-infused polymer gel dosimeter and Monte Carlo study." *Applied Radiation and Isotopes,* Vol. 141pp. 210-18, (2018).

17- Amir Ghasemi-Jangjoo and Hosein Ghiasi, "Monte Carlo study on the gold and gadolinium nanoparticles radio-sensitizer effect in the prostate I seeds radiotherapy." *Polish Journal of Medical Physics and Engineering,* Vol. 25 (No. 3), pp. 165-69, (2019).

18- Stephen J McMahon *et al.*, "Nanodosimetric effects of gold nanoparticles in megavoltage radiation therapy." *Radiotherapy and Oncology,* Vol. 100 (No. 3), pp. 412-16, (2011).

19- Stephen J McMahon *et al.*, "Energy dependence of gold nanoparticle radiosensitization in plasmid DNA." *The*

Journal of Physical Chemistry C, Vol. 115 (No. 41), pp. 20160-67, (2011).

20- Martin P Martinov, Elizabeth M Fletcher, and Rowan M Thomson, "Multiscale Monte Carlo simulations of gold nanoparticle dose-enhanced radiotherapy I: Cellular dose enhancement in microscopic models." *Medical physics,* Vol. 50 (No. 9), pp. 5853-64, (2023).

21- Keamogetswe Ramonaheng, Johannes A van Staden, and Hanlie du Raan, "Accuracy of two dosimetry software programs for 177Lu radiopharmaceutical therapy using voxel-based patient-specific phantoms." *Heliyon,* Vol. 8 (No. 7), (2022).

22- Eslam Taha, Fathi Djouider, and Essam Banoqitah, "Monte Carlo simulations for dose enhancement in cancer treatment using bismuth oxide nanoparticles implanted in brain soft tissue." *Australasian physical & engineering sciences in medicine,* Vol. 41pp. 363-70, (2018).

23- Sajad Keshavarz and Dariush Sardari, "Different distributions of gold nanoparticles on the tumor and calculation of dose enhancement factor by Monte Carlo simulation." *Nuclear Energy and Technology,* 10.3897/nucet.5.39096 Vol. 5 (No. 4), pp. 361-71, (2019).

24- M Zabihzadeh, T Moshirian, M Ghorbani, C Knaup, and MA Behrooz, "A Monte Carlo study on dose enhancement by homogeneous and inhomogeneous distributions of gold nanoparticles in radiotherapy with low energy X-rays." *Journal of biomedical physics & engineering,* Vol. 8 (No. 1), p. 13, (2018).

25- M. Zabihzadeh, T. Moshirian, M. Ghorbani, C. Knaup, and M. A. Behrooz, "A Monte Carlo Study on Dose Enhancement by Homogeneous and Inhomogeneous Distributions of Gold Nanoparticles in Radiotherapy with Low Energy X-rays." (in eng), *J Biomed Phys Eng,* Vol. 8 (No. 1), pp. 13-28, Mar (2018).

26- Chun-Hui Hsing, I. Chun Cho, Tsi-Chian Chao, Ji-Hong Hong, and Chuan-Jong Tung, "GNP enhanced responses in microdosimetric spectra for 192Ir source." *Radiation Measurements,* Vol. 118pp. 67-71, 2018/11/01/ (2018).

27- Hans Rabus, Miriam Schwarze, and Leo Thomas, "Article commentary on 'Microdosimetric and radiobiological effects of gold nanoparticles at therapeutic radiation energies' [T.M. Gray et al., IJRB 2023, 99(2), 308–317]." *International Journal of Radiation Biology,* Vol. 100 (No. 1), pp. 7-17, 2024/01/02 (2024).

28- Tara M. Gray, Shaquan David, Nema Bassiri, Devanshi Yogeshkumar Patel, Neil Kirby, and Kathryn M. Mayer, "Microdosimetric and radiobiological effects of gold nanoparticles at therapeutic radiation energies." *International Journal of Radiation Biology,* Vol. 99 (No. 2), pp. 308-17, 2023/02/01 (2023).

29- L. A. Dykman and N. G. Khlebtsov, "Gold nanoparticles in biology and medicine: recent advances and prospects." (in eng), *Acta Naturae,* Vol. 3 (No. 2), pp. 34-55, Apr (2011).